JOURNAL OF MATERIALS SCIENCE 23 (1988) 4349–4356

Y(Er)-doped tetragonal zirconia polycrystalline solid electrolyte

Part 1 *Powder processing*

P. DURAN, P. RECIO, J. R. JURADO, C. PASCUAL, C. MOURE
Departamento de Materiales Cerámicos Especiales, Instituto de Cerámica y Vidrio (CSIC), Arganda del rey, Madrid, Spain

Submicronized Y(Er)-doped zirconia powders were prepared by the hydroxide-gel precipitation method. The agglomeration state and surface of both precursors and calcined oxides are studied and are related to the compaction and sintering behaviour. The compaction response was different for the two doped zirconias which was related to the different strength of aggregates present in the powders. Although a different breakpoint in the compaction curve for each of the powders was found, the sintering behaviour was quite similar which indicates that at high compaction pressures all the aggregates were broken up and uniformly distributed in a regular packing of very fine particles. Densification during sintering seems to be governed by both the high surface activity of the powders as the driving force (below 1400° C) and the grain growth above that temperature: the shrinkage behaviour was in close agreement with the isothermal experiment results.

1. Introduction

Traditionally, ceramic materials are obtained by solid state reaction between powders. In this way a precise control of powder parameters and of the process itself becomes difficult. Furthermore, the final products so obtained have, to some extent, unpredictable properties, a wide parameter spread and a poor life expectation. During the last decade, the use of "precursors" for producing high-performance ceramic materials has become a widely accepted reliable basis, and most of the "high-technology" ceramics for new applications make use of the wet-chemical method for their preparation. Thus a very homogeneous powder with a well-defined geometrical shape and high sinterability can be achieved.

In tetragonal zirconia ceramics it is well known that the phase stability and, therefore, the properties of the fabricated materials are strongly related, among other factors, to the grain size and thus a rigorous control of the particle size of the raw starting materials become necessary. In this sense many papers [1–5] have been devoted to the study of the preparation and sintering of a stable tetragonal zirconia using different chemical routes. It is generally assumed that the sol–gel chemical route is the best method for obtaining a non-agglomerated structure powder with an extremely high sinterability. From our experience it can be pointed out that although many of the wet-chemical routes produce powders exhibiting a poor sintering behaviour, such a behaviour could be enhanced by using an adequate processing procedure. In that sense each of the processing steps should be rigorously controlled to avoid the formation of strong aggregates or agglomerates which would lead to the presence of inhomogeneities in the powder compacts and, finally, to a low density and non-uniform microstructure in the sintered bodies.

The present work was undertaken to study the different processing parameters when a combination of the two steps, hydrolysis and precipitation, according to the nature of the precursors, are present during the Y-tetragonal zirconia powder preparation. An alternative tetragonal zirconia doped with Er_2O_3, not previously reported, was also prepared.

2. Experimental procedure

2.1. Powder preparation

The ZrO_2, Y_2O_3 and Er_2O_3 raw starting materials were obtained from $Zr(C_4H_9O)_4C_4H_9OH$, $Y(NO_3)_3 \cdot 5H_2O$ and $Er(NO_3)_3 \cdot 5H_2O$, 99.9% pure, respectively. The required amount of solid yttrium or erbium nitrate was dissolved in a solution of zirconium tetrabutoxide in ethanol by stirring. This stable sol was slowly added drop-wise with vigorous stirring to a water–ammonia (12. N) solution (reverse strike). In such operating conditions a partial hydrolysis of the tetrabutoxide initially took place. Polymerization of the zirconium tetrabutoxide and a transient bulk gelation then occurred. The final step was the floculation of the gel with simultaneous coprecipitation of a very fine white powder. Mass precipitation was attained by a further addition of ammonia while stirring. Then the powder was filtered and thoroughly washed with a water–isopropyl alcohol mixture. After washing, the powder was milled and washed again with pure isopropyl alcohol. At the end of the second washing the powder was deagglomerated in a disc turbine operating at 2000 r.p.m. which provided a high liquid flow, and

0022–2461/88 $03.00 + .12

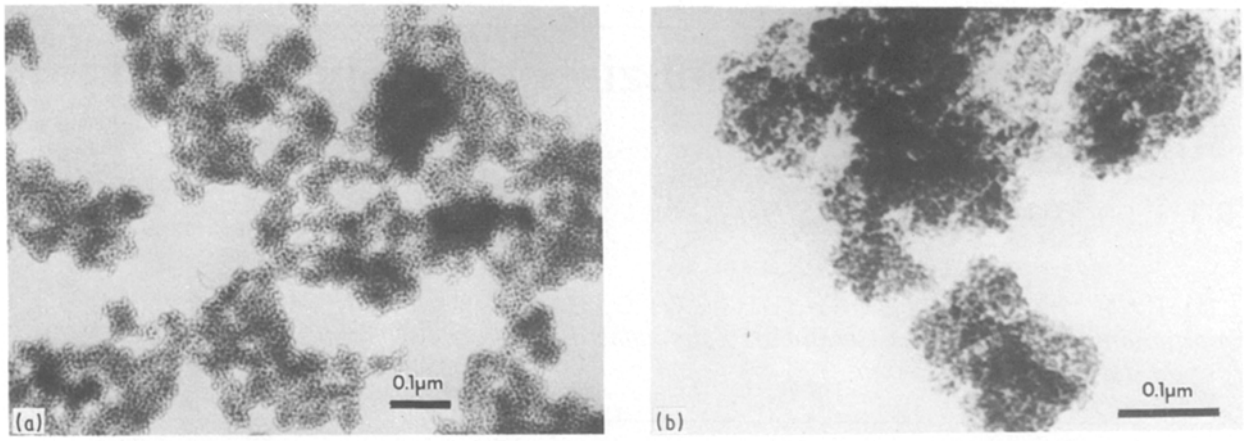

Figure 1 TEM of (a) Y-TZP and (b) Er-TZP coprecipitated powders.

enabled maximum removal of water–isopropyl from the agglomerated structure. At the same time, a strong deagglomeration of the powder could take place. After deagglomeration treatment the powder was slowly dried in a high-humidity oven at 95° C. To avoid the presence of any residual isopropyl alcohol the powder was subsequently redried at 300° C for 2 h. The powder was then calcined at 550° C for 1 h and quickly cooled in the furnace. After calcining, the powder was deagglomerated again in the disc turbine at 6000 r.p.m. for 2 min, dried and isopressed at different compaction pressures up to 350 MPa. Isothermal sintering was carried out between 900 and 1600° C in air. The shrinkage behaviour was studied using an automatic dilatometer. The Y(Er)-tetragonal zirconia polycrystalline, Y(Er)-TZP, was doped with 2 mol % Y_2O_3 (Z2Y) and 3 mol % Y_2O_3 (Z3Y), and with 2 mol % Er_2O_3 (Z2E) or 3 mol % Er_2O_3 (Z3E).

2.2. Characterization techniques

Particle size distribution in the coprecipitated powders was measured using both a coulter and a sedigraph with a lower detection limit of 0.2 μm. Specific surface areas were determined by the BET method using nitrogen as the adsorbate. The particle size and morphologies were also estimated using scanning electron microscopy (SEM) and tranmission electron microscopy (TEM). Crystallite sizes on calcined powders were determined by means of X-ray line broadening measurements [6] using a Philips X-ray diffractometer PW 1140/00 with Cu$k\alpha$ radiation. Powder compaction behaviour was studied by measuring the changes in densification with increasing isostatic pressure. The density of the sintered samples was measured by Archimedes' method. Grain growth on sintered samples was observed using SEM and grain size was measured by the interception method [7].

3. Results and discussion

3.1. Powder characterization

Powder composition was determined by chemical analysis and revealed a small deviation from starting compositions which indicates that the coprecipitation was nearly quantitative. The main impurities present were SiO_2, Al_2O_3 and Fe_2O_3 at a level lower than 400 p.p.m. TEM of the coprecipitated powders revealed the strong influence of washing and deagglomerating methods used here on both the morphology and the surface properties. Fig. 1 shows the similar morphology of the two Y-TZP and E-TZP coprecipitated zirconia powders, although the specific surface area was quite different, 240 and 190 $m^2 g^{-1}$, respectively.

The calcined powders had a high specific surface area (72 to 75 $m^2 g^{-1}$ for Y-TZP and 90 to 95 $m^2 g^{-1}$ for E-TZP), and a small crystallite size (10 to 12 nm and 8.5 to 9 nm, respectively) as measured by X-ray line broadening analysis. From transmission electron micrographs, see Fig. 2, average crystallite sizes of 9 and 7.5 nm, respectively, were measured, which are in reasonable agreement with those observations. All

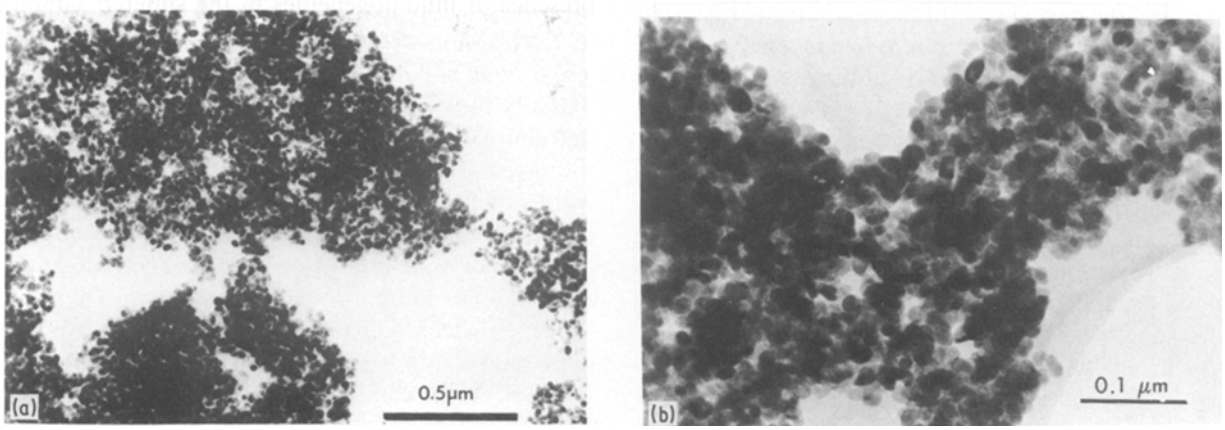

Figure 2 TEM of (a) Y-TZP and (b) Er-TZP calcined powders.

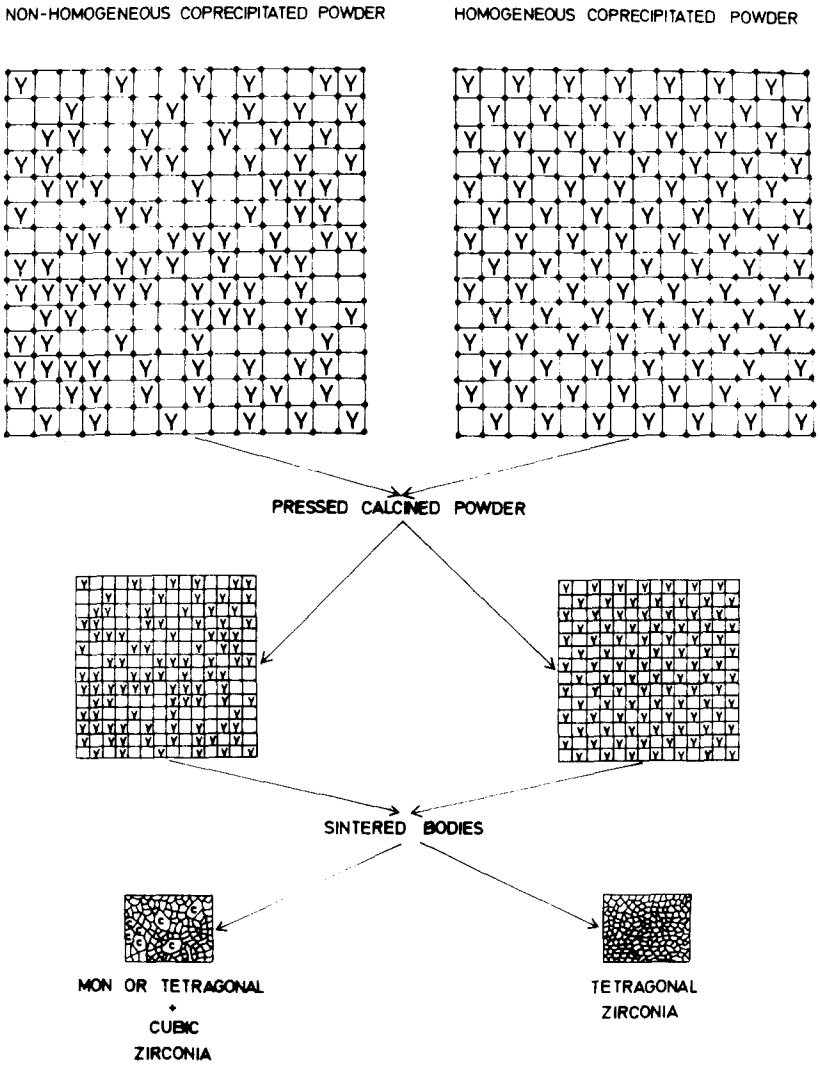

Figure 3 Schematic illustration of the influence of inhomogeneities on phase composition of the sintered bodies.

the powders observed gave direct evidence of a soft agglomerate structure, and a stronger agglomeration state was present in the case of the E-TZP powders. Such agglomerate microstructure was constituted by very small discrete particles of tetragonal zirconia which, on cooling, retained that symmetry. X-ray diffraction patterns of the calcined doped zirconia powders showed only those peaks corresponding to the tetragonal zirconia solid solution, with the following lattice parameters: $a = 0.5086 \pm 0.0005$ nm, $c = 0.5177 \pm 0.0005$ nm, and $a = 0.5080 \pm 0.0005$ nm, $c = 0.5165 \pm 0.0005$ nm in the case of 2 and 3 mol% Y-doped zirconia, respectively, and $a = 0.5088 \pm 0.0005$ nm, $c = 0.5172 \pm 0.0005$ nm, and $a = 0.5085 \pm 0.0005$ nm, $c = 0.5161 \pm 0.0005$ nm in the case of 2 and 3 mol % Er-doped zirconia, respectively.

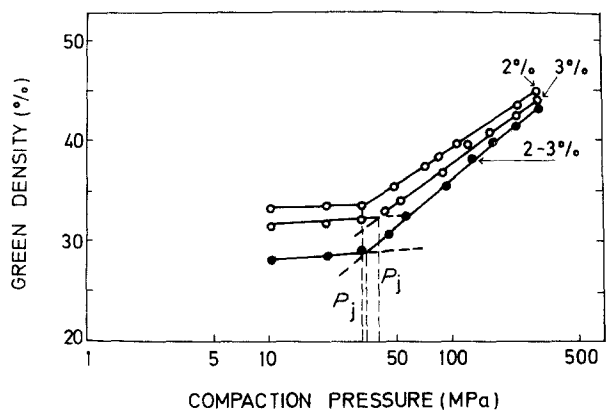

Figure 4 Compaction behaviour of the Y(Er)-TZP calcined powders. (●) Y-TZP, (○) E-TZP.

A study using EDAX analysis of the zirconium–yttrium and zirconium–erbium cation distribution in the green pressed samples showed a very uniform distribution and no compositional fluctuations were found. This result evidences the advantages of using the "reverse strike" method in the powder preparation. By using the "direct strike" method, taking into account the sequencial precipitation of the different hydroxides, the non uniform distribution of the cations in the coprecipitated powders could lead to the presence of inhomogeneities in the sintered samples, and the present phases could not be those corresponding to the original composition according to the phase equilibrium diagrams. Fig. 3 shows a schematic illustration of this influence.

3.2. Compaction response

The compaction behaviour of the calcined zirconia powders runs parallel to their agglomerate or aggregate structure. As shown in Fig. 4 in which the density values (as a percentage of the theoretical density) are plotted against the logarithm of compaction pressures, graphs with a shape as predicted by Niesz *et al.* [8] were obtained. In the low-pressure region (< 50 MPa) almost no variation in the densification as

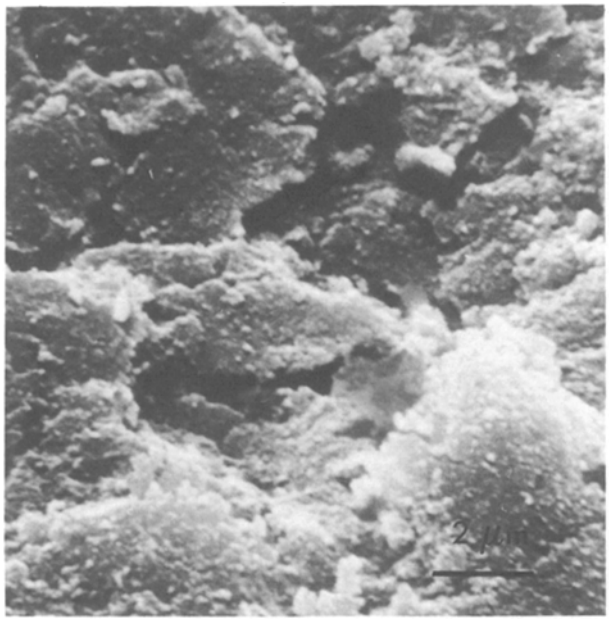

Figure 5 SEM of agglomerate structure of Er-TZP calcined powder.

a function of pressure was seen. Beyond 30 to 40 MPa, a breakpoint was found in all cases, and density increased as the pressure was increased. In view of the low compaction in the first initial linear part of the curve (< 1%), it seems probable that only rearrangement of the relatively soft agglomerates took place. The presence of some dense large agglomerates could be responsible for the increasing density in the case of E-TZP powders (see Fig. 5). In the present case two apparent agglomerate size families could be coexisting in the green microstructure of the bodies, each one having a somewhat different densification behaviour. The greater the amount of dense agglomerates, the higher the break point in the density–pressure curve which, on the other hand, is related to the compression strength of the agglomerates in the powder. The existence of a lower break point (compression strength ~ 30 MPa) in the case of the zirconia powder doped with 2 to 3 mol % Y_2O_3, was probably due to the presence of much weaker agglomerates which can be deformed more easily as a result of their lower

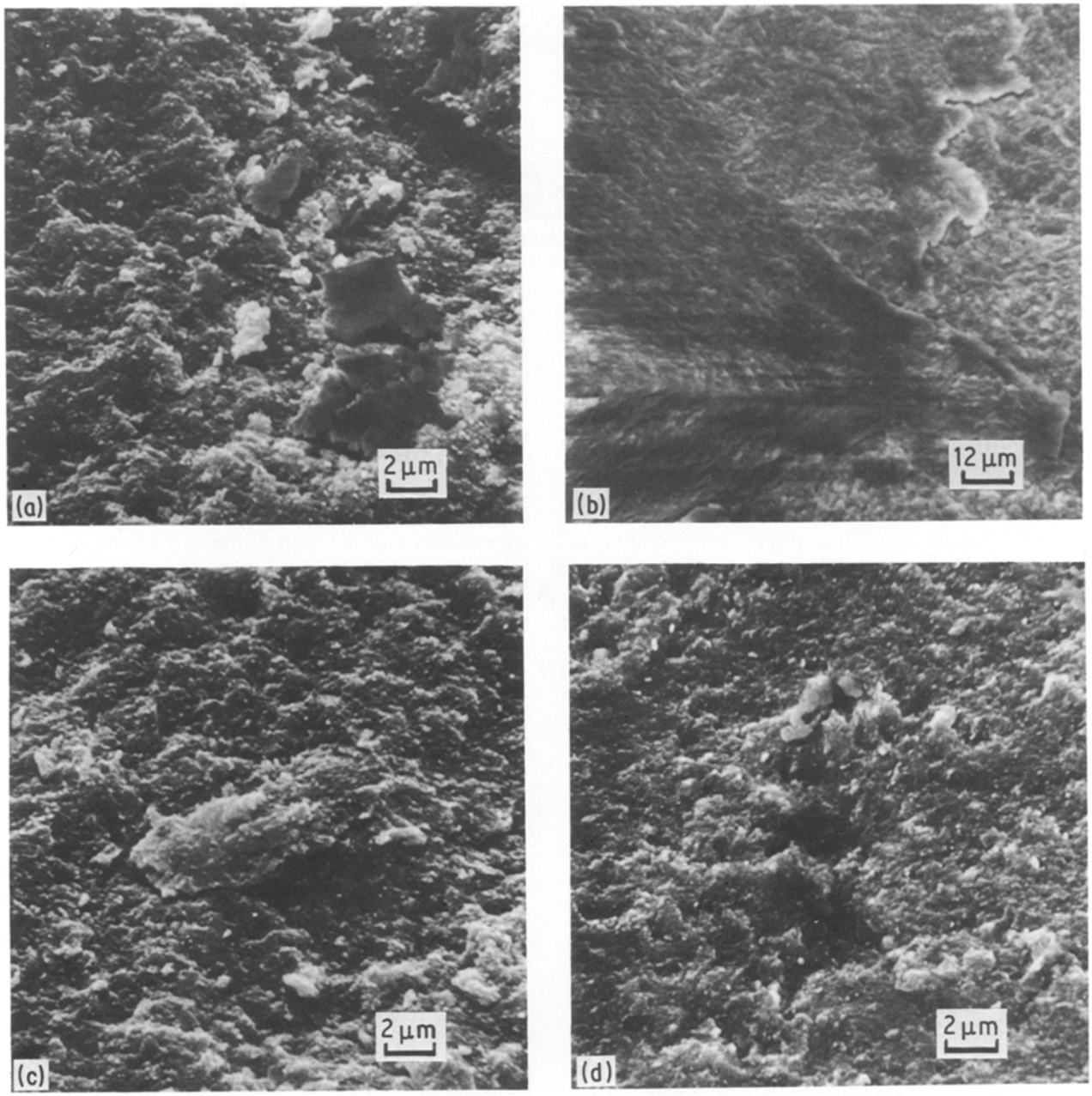

Figure 6 Microstructural evolution of the compacted bodies: (a) 20 MPa, (b) 40 MPa, (c) 80 MPa and (d) 200 MPa.

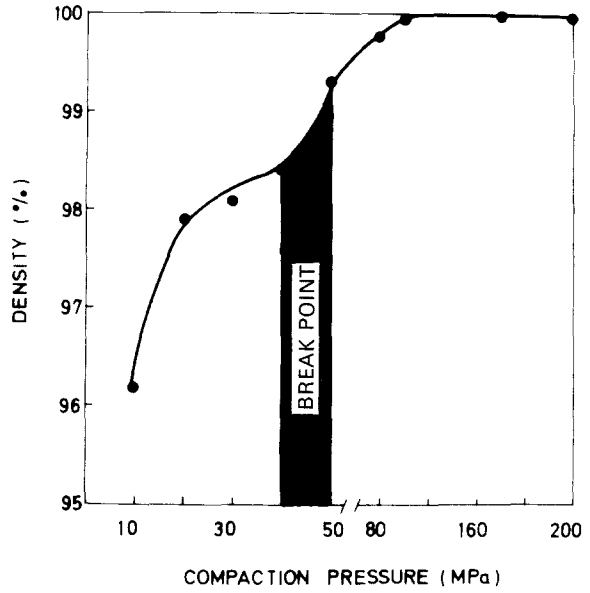

Figure 7 Density variation as a function of compaction at 1400° C for 3 mol % Er_2O_3–TZP.

strength. In all cases the compaction responses at higher pressures (> 200 MPa) was similar; however, as will be discussed later, the sintering behaviour is quite different. The present results show that compaction behaviour is strongly influenced by the individual characteristics of the agglomerates existing in the powder. An excellent paper by Van de Graaf *et al.* [9] reported a picture of the compaction sequence for YSZ, and it was considered that below the break point in the density–pressure curve, at ~ 30 MPa, a fragmentation and rearrangement of the agglomerates took place without changing their internal microstructure. In our opinion, the agglomerates could not be fragmented below that pressure but were plastically deformed and rearranged. Just at the break point pressure, agglomerate fragmentation takes place, and above that pressure, rearrangement and a stepwise compaction, which will depend on the strength of the fragmented agglomerates, was produced. Fig. 6 shows a complex picture of the microstructural development

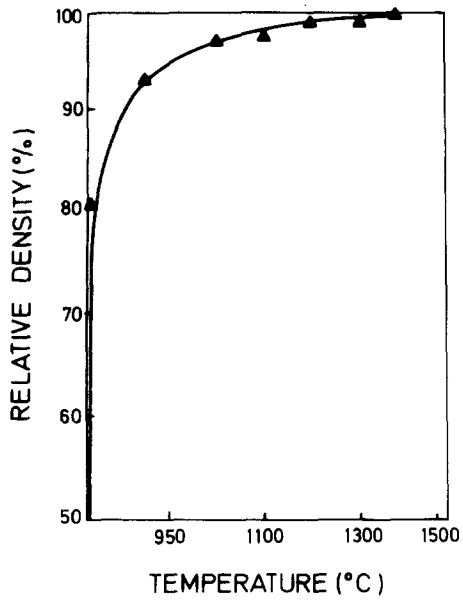

Figure 8 Densification of Er-TZP plotted against sintering temperature.

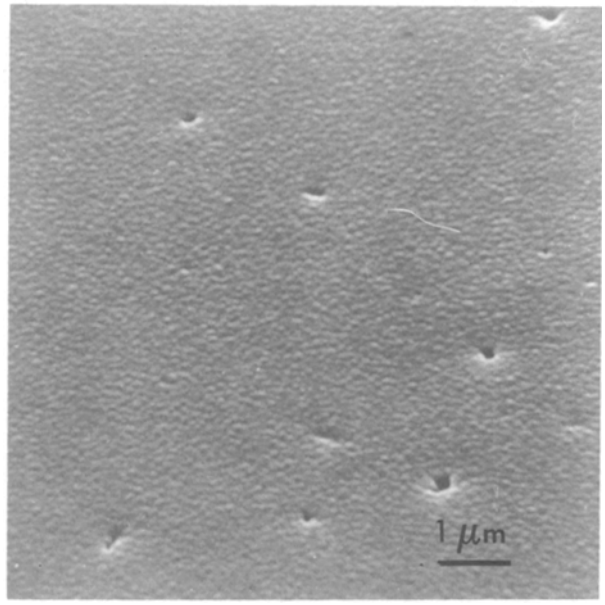

Figure 9 Microstructure of a Er-TZP (96% dense) sample.

in E-TZP for different compaction pressures. As can be seen, below the break point (< 40 MPa) the agglomerates survived and no fragmentation took place. Above 40 MPa the agglomerates were fragmented and rearranged in a uniform microstructure.

3.3. Temperature dependence of sintering

In the first part of the sintering experiments our purpose was to elucidate the influence of the compaction pressure on the sintering density. Fig. 7 shows the variation of sintering density with compaction pressure at a sintering temperature of 1400° C for 2 h. The density of the sintered bodies slowly increased as the compaction pressure was increased up to the break point in the density–pressure curve, beyond which the density rapidly increased up to the theoretical density value which was attained at a compaction pressure > 100 MPa. Taking this result into account the sintering experiments were carried out on bodies pressed at the higher compaction pressures.

The temperature dependence of sintering and microstructural development are represented in Figs 8 to 10 for Z3E. The samples exhibited a 91% density after the 950° C cycle and as high as 96% theoretical density at 1100° C for 2 h. From these results it seems reasonable to think that the turbine step before sintering the calcined powders leads to an almost total elimination of the agglomerates which improves the compaction behaviour and, therefore, the final density of the sintered bodies. Although the relative green density of the compacts (~ 47%) was very far from the theoretical value of 74% for close-packing [10], the high surface energy (93 $m^2 g^{-1}$) of the calcined powder could be a very positive factor in enhancing the driving force for rapid densification. If this is so, a rapid pore shrinkage at low temperature should be assumed. Such a rapid pore shrinkage would correspond with a fast densification at the same temperature. Fig. 9 shows the microstructure of a 96% dense sample in which some residual porosity was present. The grain size was 0.15 μm and its high

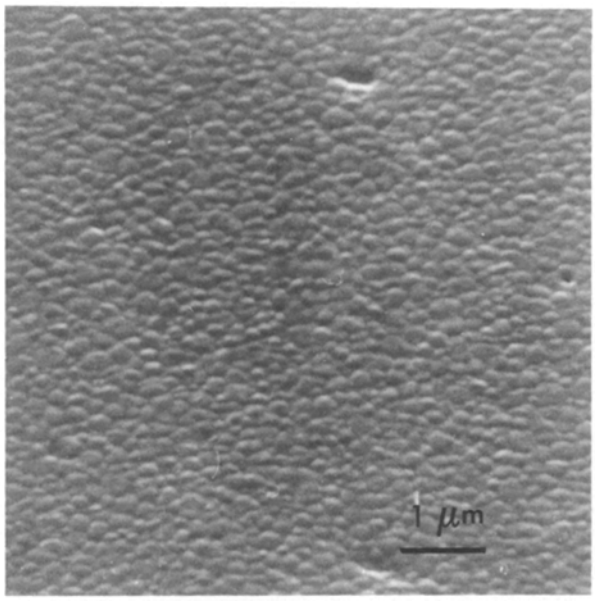

Figure 10 Microstructure of a free pore Er-TZP (99.9% dense) sample.

uniformity indicates that a normal grain growth mechanism was the dominant process. Fig. 10 shows the microstructure of a sample sintered at 1400° C for 2 h (99.9% dense). Its grain size was 0.28 μm and showed a high transparency for a thickness less than 1 mm. The very small grain growth present in these samples, and the highly uniform grain size distribution indicates that, in spite of the relatively low green density of the isopressed samples, the internal packing in the compacts was very near to the ideal situation and, in such a way, rapid migration of the pores towards the boundaries with a strong shrinkage took place in the first step of the sintering process. In this first step (below 1100° C) grain growth is hardly observed and, as a consequence, the mobility of the boundaries is very low compared to the movement rate of the pores. The non-existence of pores in the interior of the grains supported this idea. On the other hand, the high uniformity in the grain size distribution indicates the absence of aggregates in the compact microstructure and, therefore, that a normal grain growth took place during this step of the sintering process. Above 1100° C two almost simultaneous processes seem to take place: the migration of the pores along the boundaries at the same time, at which a relatively high growth of pores and grains is produced. These two processes could be considered as rate-controlling in sintering just above 1100° C. Because normal grain growth was also observed above that temperature, it could also be considered that pore migration by surface diffusion with a low pore growth took place. Such pore mobility could be, to a great extent, controlling the boundary mobility and, at the same time, the grain growth. The almost total disappearance of the residual porosity above 1100° C seems to corroborate this assumption.

Although no data for the activation energy of the sintering process are available in the present case, it could be established that in deagglomerated tetragonal zirconia compact it would be possible to achieve a final-stage sintering of 96% after 2 h at a temperature as low as 1100° C. By comparison with the data reported for the isothermal sintering of CSZ [11], it can be seen that at 1100° C our tetragonal zirconia compact could present a shrinkage rate similar to that observed for CSZ above 1600° C, and also equivalent to that found by Rhodes [12] for deagglomerated zittrite at 950° C for 1 h. These results confirm the assumption that an agglomerate-free powder can lead to a better sintering behaviour even without achieving a high green density. On the other hand, the abnormally high sintering rate found in our tetragonal zirconia compact indicates that, probably, other kinetics such as grain boundary or surface diffusions, instead of volume diffusion, could control the initial-stage sintering, although this is not a conclusive suggestion.

It must be mentioned that the sintering behaviour at temperatures higher than 1400° C was strongly dependent on the grain size in the sintered samples, and it was found that a critical grain size existed beyond which the density of the samples dramatically decreased. A detailed study of such sintering behaviour has been made and is reported in Part 2 of this series of papers [13].

3.4. Non-isothermal sintering experiments

Fig. 11a shows the CRH curves for E-TZP and Y-TZP powders isopressed at 250 MPa (green density ~ 42% theoretical density). As can be seen, the shrinkage begins at approximately 250° C and the temperature for 4% shrinkage is as low as 850° C. Shrinkage was completed below 1350° C. Fig. 11b shows the densification in terms of the relative density calculated

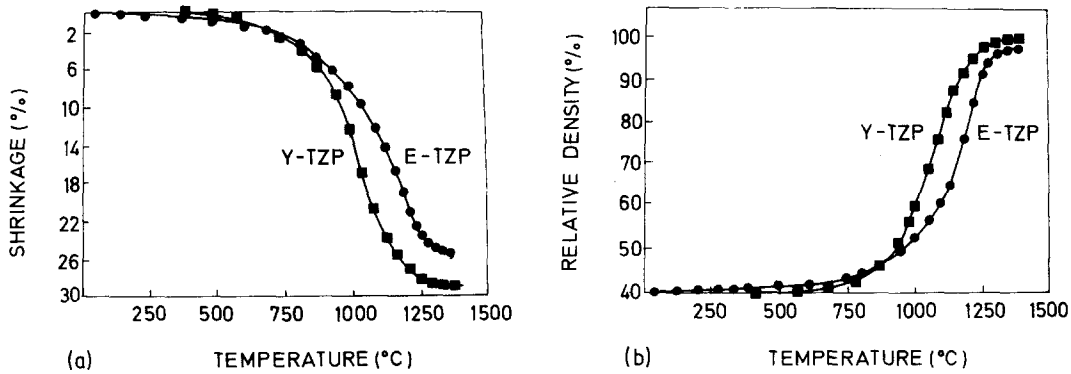

Figure 11 Non-isothermal behaviour of Y(Er)-TZP (a) shrinkage, and (b) relative density.

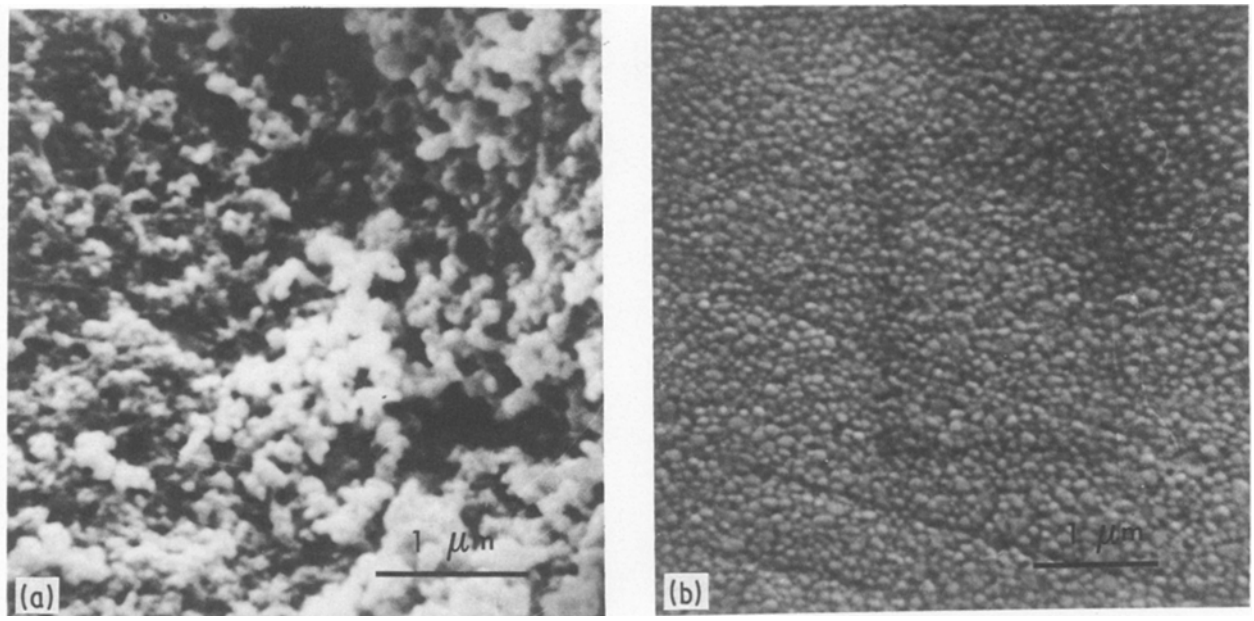

Figure 12 SEM of non-isothermally sintered samples: (a) 83% dense (fracture surface), and (b) 99.85% dense samples.

from the shrinkage data and sintered density. Up to 1080° C only a slight densification took place despite the relatively high shrinkage (~ 13%). This fact could support the view that the presence of agglomerates interferes with the initial-stage sintering. At temperatures higher than 1080° C the densification behaviour was quite different. In the short temperature interval of 150° C (between 1100 and 1250° C) a strong shrinkage was produced (~ 10%), and a rapid densification took place, attaining a final density of 99.85% below 1375° C, which agrees very well with the results obtained in the isothermal sintering experiments.

Although the very small crystallite size in both TZP powders could be a favourable factor in enhancing the driving force for densification, other parameters must be taken into account to explain such an apparently anomalous phenomenon present in the initial-stage sintering. In this way it is suggested that the fragmented agglomerates which exist in the green microstructure, being constituted by ultrafine particles probably smaller than those of the fine-grained matrix, initially shrunk more rapidly at the same time as the formation of porosity in the average microstructure of the compact. If the newly created pores are located at grain corners, further densification could continue to develop by normal sintering processes. On the other hand, if the new porosity remains in the interior of the grains its migration towards the grain boundary will be more difficult, and the densification process could be arrested. In such a case, full density could never be achieved. On the other hand, the normal grain growth process could probably be altered. If this is so, then the microstructure of the sintered samples at the end of each sintering cycle could be used as a guide to interpret the phenomena occurring in the sintered samples under study. Figs 12a and b show the microstructure of the samples sintered at 1200° C (83% dense) and at 1350° C (99.85% dense), respectively. As can be seen in the 83% dense sample, the remaining porosity was located at a grain boundary and not in the grain interior, which indicates that the densification rate of the fragmented agglomerates agrees well with that of the matrix, and no nucleus for a secondary grain growth is produced. In this case, it is shown in Fig. 12b that normal sintering and grain growth processes were present in the sintered samples. The very uniform grain size distribution obtained in the 99.85% dense sample provides evidence for a normal grain growth mechanism, which is in close agreement to Rhodes' [12] suggestions on deagglomerated sintered yttria-doped zirconia powders. Van de Graff *et al.* [14] reported a complex phenomenon picture to occur during the sintering of a deagglomerated yttria-stabilized zirconia powder. By comparison, a similar phenomenon seems to be present during the sintering of the samples studied here. However, our interpretation is quite different. Thus it cannot be assumed by us that, as the temperature was increased, all the successive steps (abnormal grain growth–normal grain growth–abnormal grain growth, leading finally to a fully densified body with a very uniform fine-grained microstructure) could be present in the global sintering process. Our experience [15] demonstrated that sintering of bodies in which such phenomena were present gave as a final result a sintered body in which full density was never achieved and, on the other hand, no uniform grain size distribution took place.

Despite the results presented here, other work is now in progress to clarify the true mechanism operating during the sintering of our deagglomerated powders. Nevertheless it seems clear at first that an adequate deagglomeration process before sintering will lead to the production of bodies with a high green density, homogeneous particle size distribution and, consequently, to improved sintering properties.

References

1. K. HABERKO, A. CIESLA and A. PROON, *Ceram. Int.* 3 (1975) 111.

2. M. A. C. G. Van de GRAAF and A. J. BURGRAAF, in "Advances in Ceramics", Vol. 12 (The American Ceramic Society, Stuttgart, 1983) pp. 744–65.
3. H. SCHUBERT, N. CLAUSSEN and M. BUHLE, *ibid.*, pp. 766–73.
4. B. FEGLEY Jr, P. WHITE and H. KENT BOWEN, *Amer. Ceram. Soc. Bull.* **64** (1985) 1115.
5. P. RECIO, C. PASCUAL, C. MOURE, J. R. JURADO and P. DURAN, *Proc. Brit. Ceram. Soc.* **38** (1986) 127.
6. K. P. KLUG and L. E. ALEXANDER, "X-ray Diffraction Procedures" (Wiley, New York, 1974).
7. R. L. FULLMAN, *Trans. AIME* **197** (1953) 447.
8. D. E. NIESZ, R. B. BENNETT and H. J. SNYDER, *Amer. Ceram. Soc. Bull.* **51** (1972) 677.
9. M. A. C. G. Van de GRAAF, J. H. H. TER MAAT and A. J. BERGRAAF, *J. Mater. Sci.* **20** (1985) 1407.
10. R. K. McGEARY, *J. Amer. Ceram. Soc.* **44** (1961) 513.
11. P. J. JORGENSEN, in "Sintering and Related Phenomena", edited by G. C. Kuczynski (Gordon and Breach, New York, 1967) pp. 401–22.
12. W. H. RHODES, *J. Amer. Ceram. Soc.* **64** (1981) 19.
13. P. DURAN, P. RECIO, J. R. JURADO, C. PASCUAL, F. CAPEL and C. MOURE, *J. Mater. Sci.* **23** (1988).
14. M. A. C. G. Van de GRAAF, J. H. H. TER MAAT and A. J. BURGRAAF, "Ceramic Powders", edited by P. Vincenzini (Elsevier, Amsterdam, 1983) pp. 983–94.
15. L. DEL OLMO, P. DURAN and C. MOURE, in "Sintering Theory and Practice", edited by D. Kolar, S. Pejovnik and M. M. Ristie (Elsevier, Amsterdam, 1982) pp. 401–8.

Received 12 October 1987
and accepted 10 February 1988